

Precursor Morphology Controlled Formation of Rutile VO₂ Nanorods and Their Self-Assembled Structure

Zhou Gui,^{*,†} Rong Fan,[‡] Weiqin Mo,[‡] Xianhui Chen,^{‡,§} Ling Yang,[†] Shuyuan Zhang,[§] Yuan Hu,[†] Zhangzhou Wang,[†] and Weicheng Fan[†]

State Key Lab of Fire Science, Department of Physics, and Structural Research Laboratory, University of Science and Technology of China, Hefei, 230026, P.R. China

Received May 29, 2002. Revised Manuscript Received September 11, 2002

Rutile VO₂ nanorods have been synthesized by the precursor morphology controlled formation. The precursor single-crystal VO₂ hydrate nanorods have been obtained via the hydrothermal reaction of KOH, V₂O₅, and hydrazine in a sealed autoclave at low temperature. The reducing agent N₂H₄ plays a key role in the control of one-dimensional morphology. According to the data of differential scanning calorimetry and thermogravimetric analysis, rutile VO₂ nanorods have been formed when the precursor VO₂ hydrate is heated at 340 °C for 1 day in flowing N₂ and maintaining the morphology of the precursor. The products have been characterized by means of X-ray powder diffraction, transmission electron microscopy, high-resolution electron microscopy, selected area electron diffraction, and X-ray energy-dispersive spectroscopy techniques. It is shown that these rutile VO₂ nanorods are self-assembled by VO₂ nanocrystalline domains with the same crystallographic direction along the rod axis. The reaction details and features are described and discussed.

Introduction

Recent progress in the synthesis and characterization of nanowires and nanorods has been driven by the need to understand the novel physical properties of one-dimensional (1-D) nanomaterials, and their potential applications in constructing nanoscale electronic and optoelectronic devices.¹ Many types of nanowires/rods have been prepared with various methods, including the vapor-phase transport,² chemical vapor deposition,³ arc discharge,⁴ laser ablation,⁵ template-based,⁶ and solution chemistry methods.⁷ Currently most of this kind of research has been focused on semiconductor systems such as CdS,⁷ GaAs,⁵ GaN,² Si,¹ ZnO,⁸ and metal nanomaterials.⁶ The present work studies an important functional oxide—rutile, VO₂, which possesses unique electrical and optical properties, leading to a wide variety of potential applications including optoelectronic switches, temperature-sensing devices,¹¹ optical switch-

ing devices,¹² modulator and polarizer of submillimeter wave radiation,¹³ optical data storage medium,¹⁴ and variable reflectance mirrors.¹⁵

Vanadium dioxide with rutile-type structure VO₂(R) has attracted much interest because it has been observed to undergo a reversible phase transition at about 68 °C.⁹ Accompanied with the phase transition, VO₂(R) shows a reversible sudden change of resistivity and a sharp change of optical transmittance.¹⁰

So far, bulk rutile-type VO₂ has been prepared by the traditional solid-state reduction process, but the size- and morphology-controlled synthesis of nanophase VO₂ via soft chemistry approaches is limited and still called for. Manthiram et al. prepared spherical VO₂(B) with average size about 100–150 nm by reducing alkali metal vanadate with borohydrides in aqueous solution, and subsequent crystallization below 300 °C. During their experiments, the transformation of VO₂(B) to VO₂(R) is sluggish, the monoclinic VO₂(R) begins to form at around 330 °C and completes at around 500 °C.¹⁶ Here we report that the precursor VO₂ hydrate nanorods can be hydrothermally synthesized with N₂H₄·H₂O as the reducing agent and templating agent. Through controlling the annealing temperature (340 °C), rutile-type VO₂(R) nanorods with the same morphology as that of vanadium oxide hydrate precursor nanorods have been

* To whom correspondence should be addressed. E-mail: zgui@ustc.edu.cn.

† State Key Lab of Fire Science.

‡ Department of Physics.

§ Structural Research Laboratory.

(1) Hu, J. T.; Odom, T. W.; Lieber, C. M. *Acc. Chem. Res.* **1999**, 32, 435.

(2) Wu, Y.; Yang, P. *Chem. Mater.* **2000**, 12, 605.

(3) Yazawa, M.; Koguchi, M.; Muto, A.; Ozawa, M.; Hiruma, K. *Appl. Phys. Lett.* **1992**, 61, 2051.

(4) Choi, Y. C.; Kim, W. S.; Park, Y. S.; Lee, S. M.; Bae, D. J.; Lee, Y. H.; Park, G. S.; Choi, W. B.; Lee, N. S.; Kim, J. M. *Adv. Mater.* **2000**, 12, 746.

(5) Morales, A. M.; Lieber, C. M. *Science* **1998**, 279, 208.

(6) Huang, M. H.; Choudrey, A.; Yang, P. *Chem. Commun.* **2000**, 12, 1063.

(7) Zhang, J. H.; Yang, X. G.; Wang, D. W.; Li, S. D.; Xie, Y.; Xia, Y. N.; Qian, Y. T. *Adv. Mater.* **2000**, 12, 1348.

(8) Huang, M. H.; Wu, Y. Y.; Feick, H.; Tran, N.; Weber, E. Yang, P. *Adv. Mater.* **2001**, 13, 113.

(9) Morin, F. J. *Phys. Rev. Lett.* **1959**, 3, 34.

(10) Rogers, K. D.; Coath, J. A.; Lovell, M. C. *J. Appl. Phys.* **1991**, 70, 1412.

(11) Takahashi, Y.; Kanamori, M.; Hashimoto, H.; Moritani, Y.; Masuda, Y. *J. Mater. Sci.* **1989**, 24, 192.

(12) Chain, E. E. *Appl. Opt.* **1991**, 30, 2782.

(13) Fan, J. C.; Fetterman, H. R.; Bachner, F. J.; Zavrasky, P. M.; Parker, C. D. *Appl. Phys. Lett.* **1977**, 30, 11.

(14) Balberb, I.; Trokman, S. *J. Appl. Phys.* **1977**, 46, 2111.

(15) Razavi, A.; Hughes, T.; Antinovitch, J.; Hoffman, J. *J. Vac. Sci. Technol.* **1989**, A7, 1310.

(16) Tsang, C.; Manthiram, A. *J. Electrochem. Soc.* **1997**, 144, 520.

synthesized. These rutile structured VO_2 nanorods are shown to be self-assembled by VO_2 nanocrystalline domains with the same crystallographic direction, nanorods also can be parallel self-assembled regularly.

Experimental Section

The following were added to a Teflon-lined stainless autoclave with capacity of 80 mL: 0.015 mol KOH, 0.005 mol V_2O_5 , and 50 mL of distilled water. After the mixture was stirred to a clear aqueous solution, 1 mL of 17% (wt %) $\text{N}_2\text{H}_4\cdot\text{H}_2\text{O}$ (0.0034 mol) was slowly added into the solution, thereby resulting in dark-colored solution due to the reduction of vanadium ion, while hydrochloric acid was added to control the pH value at 2.5–3.5. The autoclave was then sealed and heated at 150 °C for 2 days and cooled to room temperature. A pink precipitate was collected after filtration, washed with water, and dried at 80 °C for 5 h. A portion of this as-prepared VO_2 hydrate was heated at 340 °C for 1 day in a flowing N_2 atmosphere, and the color of the products changed from pink to black. The product of rutile-type $\text{VO}_2(\text{R})$ nanorods was obtained through this thermotreatment process.

X-ray powder diffraction (XRD) analysis was conducted out on a Rigaku D/Max X-ray diffractometer with graphite monochromated $\text{Cu K}\alpha$ radiation ($\lambda = 1.5418 \text{ \AA}$) to verify the formation of VO_2 hydrate and $\text{VO}_2(\text{R})$. Chemical analysis of the sample was conducted by redox titration to determine the oxidation state of vanadium. The valence difference between the oxidation states of vanadium in the sample and in completely oxidized V(VI) in VO_2^+ ions in the resulting solution could be determined by titrating the sample/ H_2SO_4 solution with a standard KMnO_4 solution.¹⁸ Transmission electron microscopy (TEM) images and selected area electron diffraction (SAED) patterns of the sample were collected on a Hitachi H-800 electron microscope operated at 200 keV. High-resolution electron microscopy (HREM) images and X-ray energy dispersion spectrum (EDS) analysis were recorded on a JEOL 2010 operated at 200 keV. Differential scanning calorimetry (DSC) and thermogravimetric (TG) analyses of the precursor sample were carried out using a Netsch STA 409C in a high-purity N_2 flowing atmosphere in a temperature range from 25 to 400 °C.

Results and Discussion

The pink as-prepared sample obtained hydrothermally was characterized by XRD analysis. The XRD pattern shown in Figure 1 indicates that the d -spacing values of all diffraction peaks are identical to those of VO_2 hydrate¹⁷ according to JCPDS card 13-346. Chemical analysis on the sample was taken by the EDS spectrum which exhibited the existence of V and O without any impurities such as elemental N or K. Redox titration¹⁸ was conducted to give direct evidence that the oxidation state of V in this sample is +3.95, very close to the theoretical value of +4. The as-prepared samples were characterized by DSC analysis (Figure 2) in a flowing N_2 atmosphere. The plot shows a broad endothermic peak centered around 231 °C corresponding to the loss of binding water and an exothermic peak at 322 °C that corresponds to a phase transition. TG analysis conducted in flowing N_2 atmosphere shows a weight loss of ~12.5% up to 280 °C, which is related to the procedure of dehydration. The above experiment results suggest we have synthesized the precursor VO_2 hydrate. The TEM images (Figure 3) reveal that the

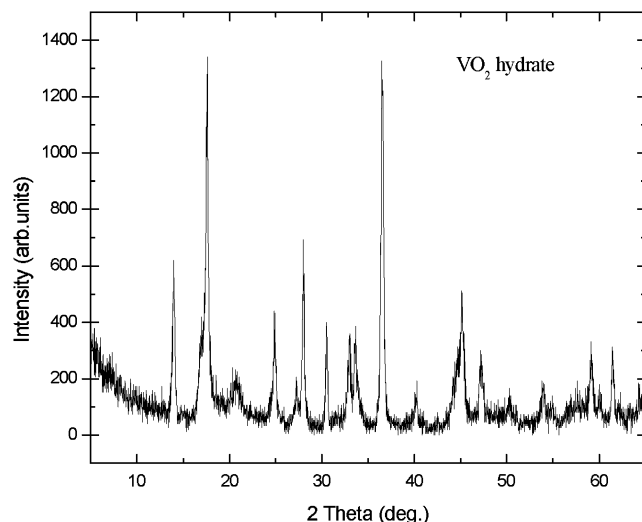


Figure 1. Powder X-ray diffraction pattern for VO_2 hydrate precursor (JCPDS 13-346).

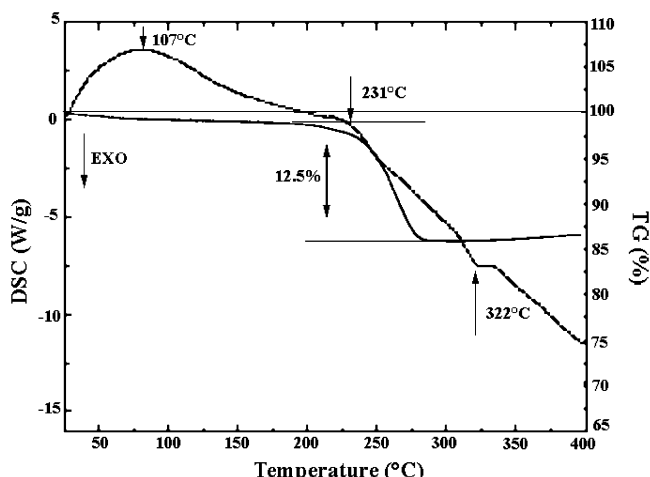


Figure 2. DSC and TG curves for the precursor VO_2 hydrate from 25 to 400 °C in a flowing N_2 atmosphere.

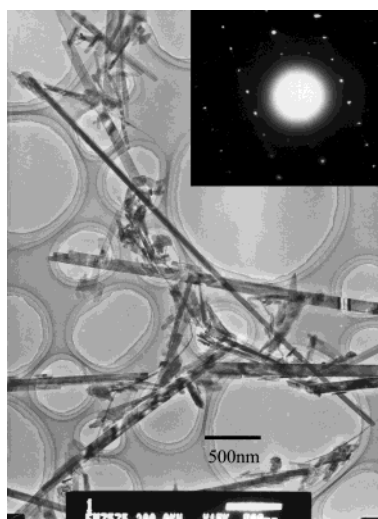


Figure 3. TEM image of the precursor VO_2 hydrate nanorods and ED pattern of single nanorod (inset).

precursor VO_2 hydrate crystallites display rodlike morphology with a uniform shape and the size is around 1–5 $\mu\text{m} \times 50\text{--}90 \text{ nm}$, and the selected area electron diffraction (SAED) pattern (inset in Figure 3) taken on

(17) Bernard, F.; Cartillier, R. *Bull. Soc. Chim. Fr.* **1961**, 1358.

(18) Gui, Z.; Fan, R.; Chen, X. H.; Wu, Y. C. *J. Solid State Chem.* **2001**, 157, 250.

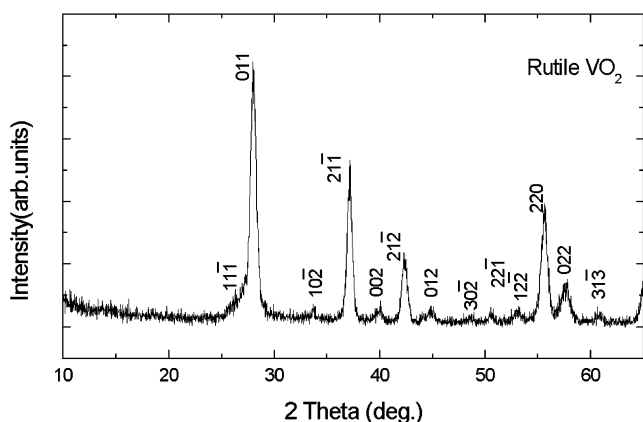


Figure 4. Powder X-ray diffraction pattern for rutile VO_2 products (JCPDS 9-142).

a single nanorod shows that all the nanorods are single crystals.

A portion of the precursor VO_2 hydrate was heated at 340 °C for 1 day in a N_2 atmosphere, and the color of the products changed from pink to black. The XRD pattern (Figure 4) of the products after heating shows the disappearance of the phase VO_2 hydrate and formation of rutile-type $\text{VO}_2(\text{R})$. The as-prepared sample was also heated at various temperatures ranging from 200 to 500 °C, but no $\text{VO}_2(\text{B})$ was detected by XRD structure analysis. This indicates that with increasing temperature, the precursor VO_2 hydrate undergoes dehydration at around 230 °C and is converted directly into rutile VO_2 completely around 320 °C, which is different from the previous reports.^{16,18}

The TEM image for the products $\text{VO}_2(\text{R})$ is shown in Figure 5a. It reveals that the products comprise $\text{VO}_2(\text{R})$ nanorods adopting the same morphology as their precursor VO_2 hydrate. These rods have average diameters of 20–30 nm and lengths of 1–5 μm . From these images it also can be seen that the nanorods are self-assembled by VO_2 nanoparticles. The high-magnification TEM images in Figure 5b show that these 1-D nanorods are composed of VO_2 nanocrystalline particles with narrow domain walls between each other regularly along the growth direction, and the selected area electron diffraction pattern on an individual particle (inset in Figure 5b) shows it is a single crystal. The diffraction spots can be indexed as (011) and (111) reflections according to the monoclinic structure of $\text{VO}_2(\text{R})$. The [011] direction of the SAED pattern is parallel to the rod axis. Extensive measurements of other single nanoparticles of these rods also show the same result, which indicates that the VO_2 nanocrystalline particles on the nanorods are self-assembled along the [011] direction (the rod axis). From the TEM image of VO_2 multi-rods (Figure 5c) it can be seen that, not only are the nanocrystalline particles self-assembled to form a single nanorod, but these nanorods are also parallelly self-assembled. The SAED pattern of many parallel assembled rods is shown inset in Figure 5c, when the electron irradiation area was adjusted to cover the entire width of all these nanorods and contained dozens of nanoparticles. The SAED pattern obtained shows the clear spots just like the nature of a bulk single crystal, which implies all the nanoparticles adopted the same crystallographic direction. The [011] direction of the SAED pattern is also parallel to the rod axis which is

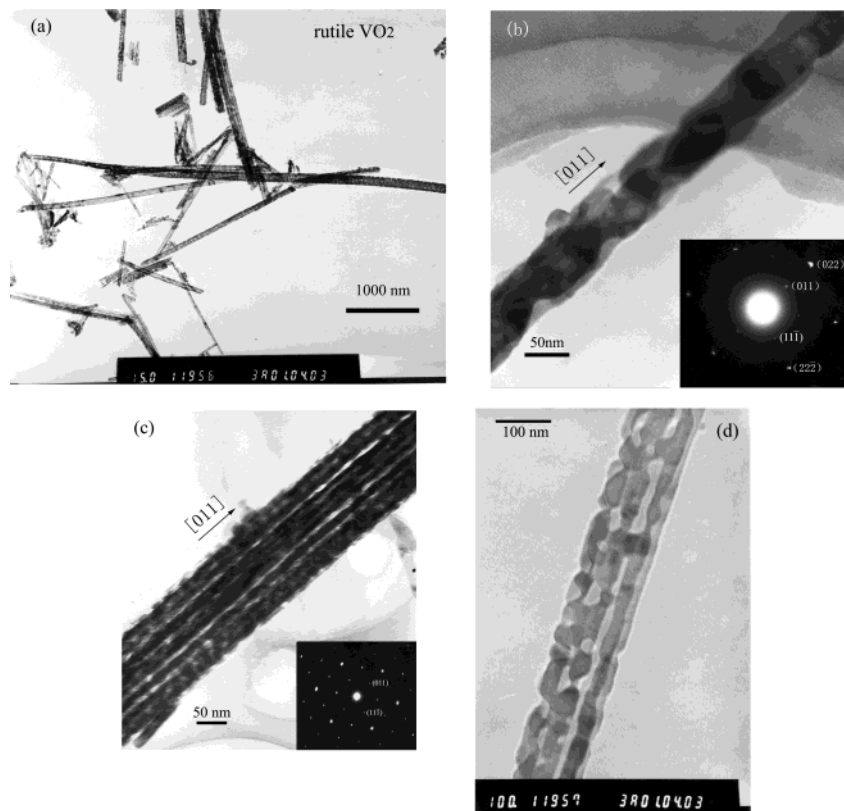


Figure 5. (a) Low-magnification TEM image of VO_2 nanorods. (b) TEM image of VO_2 single nanorod and ED pattern of an individual VO_2 nanoparticle (inset). (c) TEM image of VO_2 multiple nanorods and ED pattern of dozens of VO_2 nanoparticles (inset). (d) TEM image of VO_2 nanorods revealing nano-contact between nanoparticles.

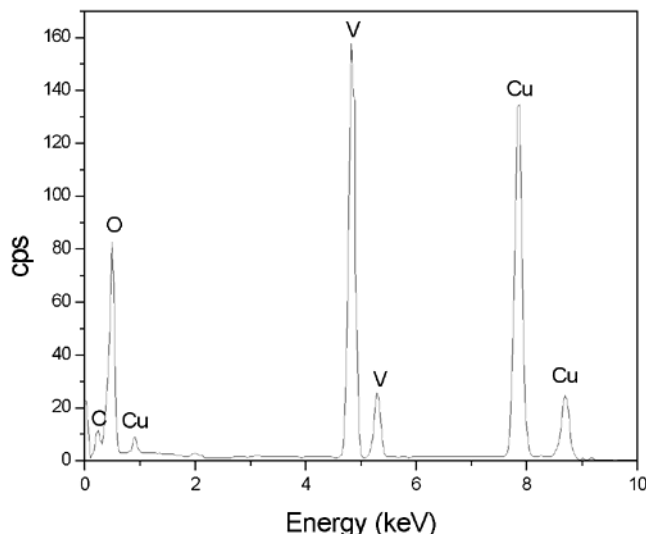


Figure 6. EDS analysis of the product rutile VO_2 . Cu peaks raised from the TEM grid.

the same as the case for an individual particle (Figure 5b). This conclusion is also demonstrated by SAED analysis on all the other nanorods assemblies.

With an elevated temperature, the precursor VO_2 hydrate is converted directly into the thermodynamically most stable rutile VO_2 . During the reaction, the single crystalline VO_2 hydrate nanorods undergo dehydration and do not damage the regular arrangement of V and O atoms. So the final product nanorods are shown to be self-assembled by VO_2 nanocrystallites with the same crystallographic direction. The TEM image of a typical product (Figure 5d) reveals that because of the loss of binding water, there is a significant shrinkage and then lots of nanocrystals form accordingly. The reason the product of rutile VO_2 still follows rodlike morphology but breaks up into many nanoparticles is that there is nano-contact between the nanoparticles. Meanwhile, the polycrystalline particles constituting VO_2 nanorods form spontaneously to stabilize the structure mechanically against collapse during binding water removal.

Chemical analysis on the nanorods was taken by EDS spectrum (Figure 6) which exhibits the existence of V and O without any impurities such as elemental N and K. The samples of vanadium dioxide were found to be unstable under irradiation by a strong electron beam; high-resolution electron microscopy (HREM) images were taken immediately after switching on the electron beam. The HREM images (Figure 7) show the clear lattice fringes with spacing of 3.18 Å between adjacent lattice planes corresponding to the distance between two (011) crystal planes of VO_2 . The result is consistent with the SAED patterns of Figure 5.

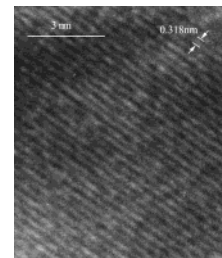


Figure 7. High-resolution TEM image of VO_2 nanorods showing the lattice fringes.

We found that the formation of the precursor VO_2 hydrate strongly depends on the chemical reaction conditions, especially the temperature and the pH value of solution. The pH value within the narrow range of 2.5–3.5 favors the formation of the pure precursor VO_2 hydrate. When the pH value is larger than about 3.5, only black $\text{K}_x\text{V}_2\text{O}_5$ powder is obtained. When the reaction temperature is higher than 160 °C, other vanadium compounds are found in the product. Much shorter nanorods (15 × 200 nm) are obtained at 110 °C. After annealing at 340 °C, VO_2 shorter nanorods have formed with the same morphology as their hydrate precursor. The optimum condition for preparing the precursor VO_2 hydrate with longer nanorods should be at 150 °C with pH value of 2.5–3.5. The reducing agent N_2H_4 is used not only to generate a reducing atmosphere for the formation of reduced VO_2 hydrate, but perhaps also plays a key role like a soft template in the control of 1-dimensional morphology as demonstrated in a previous report¹⁸ because N_2H_4 can also serve as a good coordination agent for central vanadium ions.

Conclusions

In summary, we have successfully synthesized 1-D $\text{VO}_2(\text{R})$ nanorods, which are self-assembled by $\text{VO}_2(\text{R})$ nanocrystalline particles with the same crystallographic growth direction along the rod axis and have the same morphology as their precursor VO_2 hydrate. The synthesis of these $\text{VO}_2(\text{R})$ nanorods with lengths of more than a few micrometers accordingly provides a chance to explore the size effect of 1-D $\text{VO}_2(\text{R})$ nanostructure with nano-contact between each other and the same crystallographic growth direction of each nanoparticle on their electrical and optical properties, especially the electron transport and optoconductivity through an individual nanorod. It also makes it possible to fabricate functional nano-devices using these 1-D $\text{VO}_2(\text{R})$ nanorods as building blocks.

Acknowledgment. This work was supported by a grant from the Natural Science Foundation of China (50003008) and China NKBRSF project 2001CB409600.

CM020178F